

H<sub>2</sub>O<sub>2</sub>-Reactivity of Copper(II) Complexes Supported by Tris[(pyridin-2-yl)methyl]amine Ligands with 6-Phenyl SubstituentsAtsushi Kunishita,<sup>†</sup> Minoru Kubo,<sup>‡</sup> Hirohito Ishimaru,<sup>‡</sup> Takashi Ogura,<sup>‡</sup> Hideki Sugimoto,<sup>†</sup> and Shinobu Itoh<sup>\*,†,§,⊥</sup>

Department of Material and Life Science, Division of Advanced Science and Biotechnology, Graduate School of Engineering, Osaka University, 2-1 Yamadaoka, Suita, Osaka 565-0871, Japan, Department of Chemistry, Graduate School of Science, Osaka City University, 3-3-138 Sugimoto, Sumiyoshi-ku, Osaka 558-8585, Japan, Institute for Molecular Science, National Institutes of Natural Sciences, 38 Nishigo-Naka, Myodaiji, Okazaki 444-8585, Japan, and Research Institute of Picobiology, Graduate School of Life Science, University of Hyogo, 3-2-1 Kouto, Kamigori-cho, Ako-gun, Hyogo 678-1297, Japan

Received August 17, 2008

The structure and H<sub>2</sub>O<sub>2</sub>-reactivity of a series of copper(II) complexes supported by tris[(pyridin-2-yl)methyl]amine (TPA) derivatives having a phenyl group at the 6-position of pyridine donor group(s) [(6-phenylpyridin-2-yl)methyl]bis[(pyridin-2-yl)methyl]amine (Ph<sub>1</sub>TPA), bis[(6-phenylpyridin-2-yl)methyl][(pyridin-2-yl)methyl]amine (Ph<sub>2</sub>TPA), and tris[(6-phenylpyridin-2-yl)methyl]amine (Ph<sub>3</sub>TPA) have systematically been examined to get insights into the aromatic substituent (6-Ph) effects on the coordination chemistry of TPA ligand system. The X-ray crystallographic analyses have revealed that [Cu<sup>II</sup>(TPA)(CH<sub>3</sub>CN)](ClO<sub>4</sub>)<sub>2</sub> (**CuTPA**) and [Cu<sup>II</sup>(Ph<sub>3</sub>TPA)(CH<sub>3</sub>CN)](ClO<sub>4</sub>)<sub>2</sub> (**3**) exhibit a trigonal bipyramidal structure, whereas [Cu<sup>II</sup>(Ph<sub>1</sub>TPA)(CH<sub>3</sub>CN)](ClO<sub>4</sub>)<sub>2</sub> (**1**) shows a slightly distorted square pyramidal structure and [Cu<sup>II</sup>(Ph<sub>2</sub>TPA)(CH<sub>3</sub>CN)](ClO<sub>4</sub>)<sub>2</sub> (**2**) has an intermediate structure between trigonal bipyramidal and square pyramidal. On the other hand, the UV–vis and ESR data have suggested that all the copper(II) complexes have a similar trigonal bipyramidal structure in solution. The redox potentials of **CuTPA**, **1**, **2**, and **3** have been determined as  $E_{1/2} = -0.34, -0.28, -0.16,$  and  $-0.04$  mV vs Ag/AgNO<sub>3</sub>, respectively, demonstrating that introduction of each 6-Ph group causes positive shift of  $E_{1/2}$  about 0.1 V. Notable difference in H<sub>2</sub>O<sub>2</sub>-reactivity has been found among the copper(II) complexes. Namely, **CuTPA** and **1** afforded mononuclear copper(II)-hydroperoxo complexes **CuTPA-OOH** and **1-OOH**, respectively, whereas complex **2** provided bis( $\mu$ -oxo)dicopper(III) complex **2-oxo**. On the other hand, copper(II) complex **3** was reduced to the corresponding copper(I) complex **3<sup>red</sup>**. On the basis of the H<sub>2</sub>O<sub>2</sub>-reactivity together with the X-ray structures and the redox potentials of the copper(II) complexes, the substituent effects of 6-Ph are discussed in detail.

## Introduction

TPA, tris[(pyridin-2-yl)methyl]amine, is one of the most popular tetradentate tripodal ligands in coordination chemistry.<sup>1,2</sup> A large number of transitional metal complexes of

this ligand have been prepared, and their structure, physicochemical properties, and reactivity have been explored in detail.<sup>1,2</sup> Recently, several types of TPA derivatives have also been developed to tune the structure and properties of the supported complexes, where steric constraints and/or electronic effects induced by the substituents are crucial.<sup>1–9</sup> For instance, Suzuki, Tanaka, and co-workers systematically investigated the structures and the redox properties of

\* To whom correspondence should be addressed. E-mail: shinobu@mls.eng.osaka-u.ac.jp.

<sup>†</sup> Osaka City University.

<sup>‡</sup> University of Hyogo.

<sup>§</sup> Osaka University.

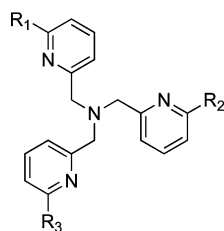
<sup>⊥</sup> Institute for Molecular Science.

(1) (a) Berreau, L. M. *Comments Inorg. Chem.* **2007**, *28*, 123–171. (b) Ingle, G. K.; Watkins, R. W.; Arif, A. M.; Berreau, L. M. *J. Coord. Chem.* **2008**, *61*, 61–77.

(2) Blackman, A. G. *Eur. J. Inorg. Chem.* **2008**, *17*, 2633–2647.

(3) (a) Karlin, K. D.; Kaderli, S.; Zuberbuhler, A. D. *Acc. Chem. Res.* **1997**, *30*, 139–147. (b) Kope, M.-A.; Karlin, K. D. In *Biomimetic Oxidations Catalyzed by Transition Metal Complexes*; Meunier, B., Ed.; Imperial College Press: London, 2000; pp 309–362. (c) Hatcher, L. Q.; Karlin, K. D. *J. Biol. Inorg. Chem.* **2004**, *9*, 669–683.

Chart 1



R <sub>1</sub>	R <sub>2</sub>	R <sub>3</sub>	Ligand	Cu <sup>II</sup> -complex
H	H	H	TPA	<b>CuTPA</b>
Me	H	H	Me <sub>1</sub> TPA	
Me	Me	H	Me <sub>2</sub> TPA	
Me	Me	Me	Me <sub>3</sub> TPA	
Ph	H	H	Ph <sub>1</sub> TPA	<b>1</b>
Ph	Ph	H	Ph <sub>2</sub> TPA	<b>2</b>
Ph	Ph	Ph	Ph <sub>3</sub> TPA	<b>3</b>

[Cu<sup>II</sup>(Me<sub>n</sub>TPA)(Cl)]<sup>+</sup> (Me<sub>n</sub>TPA, *n* = 1–3, see Chart 1) to find that structural perturbation induced by the 6-Me substituent(s) leads to positive shift of the redox potential of the copper(II) complexes (*E*<sub>1/2</sub> = −0.33, −0.20, and −0.04 mV vs Ag/AgCl, respectively, in H<sub>2</sub>O (pH 7)).<sup>10</sup> The results have been attributed mainly to steric repulsion between the 6-methyl substituent and the bound metal ion, which causes reduction of electron-donor ability of the pyridine donor groups.<sup>10</sup> Such effects of the 6-Me group(s) of Me<sub>n</sub>TPA have also been evaluated in the iron system, by which not only *E*<sub>1/2</sub> but also the spin state of the metal center can be altered to control the reactivity of the supported iron complexes.<sup>4</sup>

More recently, TPA ligands with 6-Ph substituent(s) (Ph<sub>n</sub>TPA, Chart 1) have also been investigated in anticipation of larger and/or different types of effects on the coordination chemistry of TPA. For instance, Canary and co-workers have examined the substituent effects of the 6-Ph groups on the structures and redox properties of Cu(I) and Cu(II) complexes using Ph<sub>3</sub>TPA (Chart 1), where the 6-Ph substituents causes a positive shift of the redox potential by 300–480 mV relative to that of the copper(II) complex of TPA itself depending on the solvent used.<sup>11</sup> The positive shift of the redox potential has been attributed to an electron withdrawing effect by 6-Ph and a reduction of the local dielectric character because of steric shielding in the metal center.<sup>11</sup> However, little has been discussed about the aromatic substituent effects on the reactivity of Ph<sub>n</sub>TPA complexes. In this study, we have systematically investigated the Cu(II)-H<sub>2</sub>O<sub>2</sub> reactivity in the Ph<sub>n</sub>TPA ligand system to disclose the aromatic substituent effects on the redox reactivity of the copper-TPA complexes.

It has been reported that the reaction of the copper(II) complex of TPA and H<sub>2</sub>O<sub>2</sub> gives a mononuclear copper(II)

hydroperoxo complex LCu<sup>II</sup>-OOH,<sup>12</sup> which is one of the important active oxygen intermediates involved in copper oxidases and copper monooxygenases as well as in numerous copper-catalyzed oxidation reactions.<sup>13</sup> Karlin and his co-workers have recently demonstrated that the LCu<sup>II</sup>-OOH intermediate generated by using a Ph<sub>1</sub>TPA derivative having a *p*-*tert*-butyl group on 6-Ph has an ability to induce an aromatic ligand hydroxylation in acetone.<sup>14</sup> Here we have found that the copper(II) complexes supported by Ph<sub>2</sub>TPA and Ph<sub>3</sub>TPA exhibit totally different reactivity toward H<sub>2</sub>O<sub>2</sub>, providing more insights into the substituent effects on the TPA coordination chemistry.

## Experimental Section

**General Procedures.** The reagents and the solvents used in this study, except the ligand and the copper complexes, were commercial products of the highest available purity and were further purified by the standard methods, if necessary.<sup>15</sup> Ligands TPA and Ph<sub>n</sub>TPA were synthesized according to the reported procedures.<sup>11,16–18</sup> The copper(II) complexes of [Cu<sup>II</sup>(TPA)(CH<sub>3</sub>CN)](ClO<sub>4</sub>)<sub>2</sub> (**CuTPA**) and [Cu<sup>II</sup>(Ph<sub>3</sub>TPA)(CH<sub>3</sub>CN)](ClO<sub>4</sub>)<sub>2</sub> (**3**) were prepared as reported previously.<sup>11,12</sup> FT-IR spectra were recorded on a Jasco FTIR-4100, and UV–visible spectra were taken on a Jasco V-570 or a Hewlett-Packard 8453 photo diode array spectrophotometer equipped with a Unisoku thermostatted cell holder USP-203. <sup>1</sup>H NMR spectra were recorded on a JEOL FT-NMR Lambda 300WB. Electron spin resonance (ESR) spectra were recorded on a Bruker E-500 spectrometer at −150 °C. Mass spectra were recorded on a JEOL JMS-AX500 mass spectrometer and JMS-700T Tandem MS-station mass spectrometer. ESI-MS (electrospray ionization mass spectra) measurements were performed on a PE SCIEX API 150EX or a Micromass LCT spectrometer. Resonance Raman scattering was excited at 406.7 nm from a Kr<sup>+</sup> laser (Spectra Physics, BeamLok 2060). Resonance Raman scattering was dispersed by a single

- (4) (a) Costas, M.; Mehn, M. P.; Jensen, M. P.; Que, L., Jr. *Chem. Rev.* **2004**, *104*, 939–986. (b) Shan, X.; Que, L., Jr. *J. Inorg. Biochem.* **2006**, *100*, 421–433. (c) Que, L., Jr. *Acc. Chem. Res.* **2007**, *40*, 493–500.
- (5) Suzuki, M. *Acc. Chem. Res.* **2007**, *40*, 609–617.
- (6) Yamaguchi, S.; Masuda, H. *Sci. Technol. Adv. Mater.* **2005**, *6*, 34–47.
- (7) Tshuva, E. Y.; Lippard, S. J. *Chem. Rev.* **2004**, *104*, 987–1012.
- (8) Mirica, L. M.; Ottenwaelde, X.; Stack, T. D. P. *Chem. Rev.* **2004**, *104*, 1013–1045.
- (9) Lewis, E. A.; Tolman, W. B. *Chem. Rev.* **2004**, *104*, 1047–1076.
- (10) Nagao, H.; Komeda, N.; Mukaida, M.; Suzuki, M.; Tanaka, K. *Inorg. Chem.* **1996**, *35*, 6809–6815.
- (11) (a) Chuang, C.-L.; Lim, K. T.; Chen, Q.; Zubieta, J.; Canary, J. W. *Inorg. Chem.* **1995**, *34*, 2562–2568. (b) Chuang, C.-L.; Lim, K. T.; Canary, J. W. *Supramol. Chem.* **1995**, *5*, 39–43.

- (12) Fujii, T.; Naito, A.; Yamaguchi, S.; Wada, A.; Funahashi, Y.; Jitsukawa, K.; Nagatomo, S.; Kitagawa, T.; Masuda, H. *Chem. Commun.* **2003**, 2700–2701.
- (13) Itoh, S. *Curr. Opin. Chem. Biol.* **2006**, *10*, 115–122.
- (14) Maiti, D.; Lucas, H. R.; Sarjeant, A. A. N.; Karlin, K. D. *J. Am. Chem. Soc.* **2007**, *129*, 6998–6999.
- (15) Armarego, W. L. F.; Perrin, D. D. In *Purification of Laboratory Chemicals*, 4th ed.; Butterworth-Heinemann: Oxford, 1996; pp 176 and 215.
- (16) Tyeklar, Z.; Jacobson, R. R.; Wei, N.; Murthy, N. N.; Zubieta, J.; Karlin, K. D. *J. Am. Chem. Soc.* **1993**, *115*, 2677–2689.
- (17) Jensen, M. P.; Que, E. L.; Shan, X.; Rybak-Akimova, E.; Que, L., Jr. *Dalton. Trans.* **2006**, 3523–3527.
- (18) Makowska-Grzyska, M. M.; Szajna, E.; Shipley, C.; Arif, A. M.; Mitchell, M. H.; Halfen, J. A.; Berreau, L. M. *Inorg. Chem.* **2003**, *42*, 7472–7488.

polychromator (Ritsu Oyo Kogaku, MC-100) and was detected by a liquid nitrogen cooled CCD detector (Roper Scientific, LNCDD-1100-PB). The resonance Raman measurements were carried out using a rotated cylindrical cell thermostatted at  $-80\text{ }^{\circ}\text{C}$  or a rotating NMR tube (outer diameter = 5 mm) thermostatted at  $-40\text{ }^{\circ}\text{C}$  by flashing cold nitrogen gas. A  $135^{\circ}$  back-scattering geometry was used. Cyclic voltammetric measurements were performed on an ALS-630A electrochemical analyzer in deaerated  $\text{CH}_3\text{CN}$  containing 0.10 M  $\text{NBu}_4\text{ClO}_4$  as a supporting electrolyte. A Pt working electrode (BAS) was polished with BAS polishing alumina suspension and rinsed with acetone before use. The counter electrode was a platinum wire. The measured potentials were recorded with respect to a  $\text{Ag}/\text{AgNO}_3$  (0.01 M) reference electrode. All electrochemical measurements were carried out in a glovebox filled with Ar gas at  $25\text{ }^{\circ}\text{C}$ . Elemental analyses were recorded with a Perkin-Elmer or a Fisons instruments EA1108 Elemental Analyzer.

**Synthesis of Copper(II) Complexes.** *Caution! The perchlorate salts in this study are all potentially explosive and should be handled with care.*

**$[\text{Cu}^{\text{II}}(\text{Ph}_1\text{TPA})(\text{CH}_3\text{CN})](\text{ClO}_4)_2$  (**1**).**  $\text{Cu}^{\text{II}}(\text{ClO}_4)_2 \cdot 6\text{H}_2\text{O}$  (148.0 mg, 0.40 mmol) was added to a  $\text{CH}_3\text{CN}$  solution (5 mL) of ligand  $\text{Ph}_1\text{TPA}$  (146.4 mg, 0.40 mmol). After stirring for 10 min at room temperature, insoluble material was removed by filtration. Addition of ether (100 mL) to the filtrate gave a blue powder that was precipitated by standing the mixture for several minutes. The supernatant was then removed by decantation, and the remained blue solid was washed with ether three times and dried to give complex **1** in 69%. Single crystals of **1** were obtained by vapor diffusion of ether into a  $\text{CH}_3\text{CN}$  solution of the complex. FT-IR (KBr) 1109, 1094, and  $623\text{ cm}^{-1}$  ( $\text{ClO}_4^-$ ); HR-MS (FAB, pos.)  $m/z = 429.1145$  calcd for  $\text{C}_{24}\text{H}_{22}\text{N}_4\text{Cu}$ ; 429.1140; Anal. Calcd for  $[\text{Cu}^{\text{II}}(\text{Ph}_1\text{TPA})(\text{CH}_3\text{CN})](\text{ClO}_4)_2$  ( $\text{C}_{26}\text{H}_{25}\text{CuCl}_2\text{N}_5\text{O}_8$ ): C, 46.61; H, 3.76; N, 10.45. Found: C, 46.64; H, 3.69; N, 10.32.

**$[\text{Cu}^{\text{II}}(\text{Ph}_2\text{TPA})(\text{CH}_3\text{CN})](\text{ClO}_4)_2$  (**2**).** This compound was prepared by following the same procedures as described for **1** in 89%. Single crystals of **2** were obtained by vapor diffusion of ether into a  $\text{CH}_3\text{CN}$  solution of the complex. FT-IR (KBr) 1091 and  $623\text{ cm}^{-1}$  ( $\text{ClO}_4^-$ ); HR-MS (FAB, pos.)  $m/z = 505.1448$  calcd for  $\text{C}_{30}\text{H}_{26}\text{N}_4\text{Cu}$ ; 505.1453; Anal. Calcd for  $[\text{Cu}^{\text{II}}(\text{Ph}_2\text{TPA})(\text{CH}_3\text{CN})](\text{ClO}_4)_2 \cdot 0.5\text{H}_2\text{O}$  ( $\text{C}_{21}\text{H}_{31}\text{CuCl}_2\text{N}_4\text{O}_{8.5}$ ): C, 50.90; H, 4.00; N, 9.28. Found: C, 50.62; H, 3.81; N, 9.27.

**$[\text{Cu}^{\text{II}}_2(\text{Ph}_2\text{TPA})_2(\mu\text{-OH})_2](\text{CF}_3\text{SO}_3)_2$  (**4**).**  $\text{Cu}^{\text{II}}(\text{CF}_3\text{SO}_3)_2$  (109.0 mg, 0.30 mmol) and  $\text{Et}_3\text{N}$  (1 eq) were added to an MeOH solution (2 mL) of ligand  $\text{Ph}_2\text{TPA}$  (132.6 mg, 0.30 mmol). After stirring the solution for 10 min at room temperature, insoluble material was removed by filtration. Addition of ether (100 mL) to the filtrate gave blue powder that was precipitated by standing the mixture for several minutes. The supernatant was then removed by decantation, and the remaining blue solid was washed with ether three times and dried to give complex **4** in 71%. Single crystals of **4** were obtained by vapor diffusion of ether into a  $\text{CH}_3\text{CN}$  solution of the complex. FT-IR (KBr)  $3600\text{ cm}^{-1}$  ( $\text{OH}^-$ ), 1222, 1165, 1032, and  $638\text{ cm}^{-1}$  ( $\text{CF}_3\text{SO}_3^-$ ); ESI-MS (pos.)  $m/z = 523.4$   $[\text{Cu}^{\text{II}}(\text{Ph}_2\text{TPA})(\text{OH})]^+$  and  $m/z = 1193.5$   $[\text{Cu}^{\text{II}}_2(\text{Ph}_2\text{TPA})_2(\mu\text{-OH})_2(\text{CF}_3\text{SO}_3)]^+$ ; Anal. Calcd for  $[\text{Cu}^{\text{II}}_2(\text{Ph}_2\text{TPA})_2(\mu\text{-OH})_2](\text{CF}_3\text{SO}_3)_2 \cdot \text{H}_2\text{O}$  ( $\text{C}_{62}\text{H}_{56}\text{Cu}_2\text{F}_6\text{N}_8\text{O}_9\text{S}_2$ ): C, 54.66; H, 4.14; N, 8.22. Found: C, 54.62; H, 4.03; N, 8.19.

**X-ray Structure Determination.** Each single crystal was mounted on a glass-fiber. Data of X-ray diffraction were collected by a Rigaku RAXIS-RAPID imaging plate two-dimensional area detector using graphite-monochromated Mo  $\text{K}\alpha$  radiation ( $\lambda = 0.71069\text{ \AA}$ ) to  $2\theta_{\text{max}}$  of  $55^{\circ}$ . All the crystallographic calculations were performed by using the Crystal Structure software package

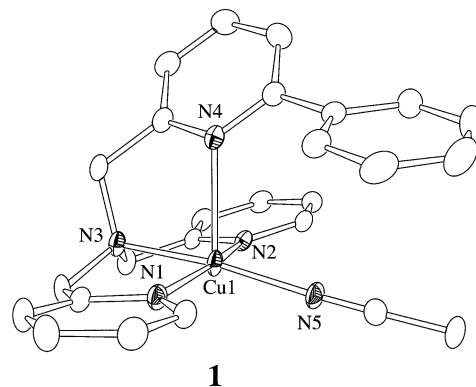


**Figure 1.** Oak Ridge Thermal Ellipsoid Plot (ORTEP) drawing of **1** showing 50% probability thermal ellipsoids. The counteranion and the hydrogen atoms are omitted for clarity.

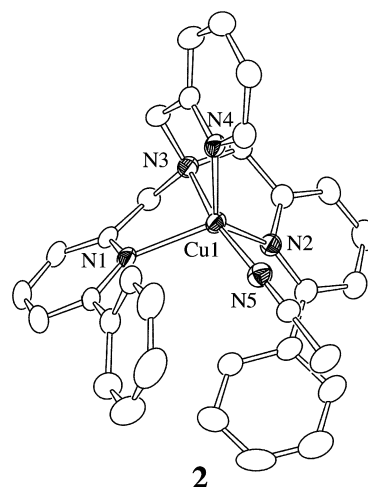


**Figure 2.** ORTEP drawing of **2** showing 50% probability thermal ellipsoids. The counteranion and the hydrogen atoms are omitted for clarity.

of the Molecular Structure Corporation [Crystal Structure: Crystal Structure Analysis Package version 3.8.1, Molecular Structure Corp. and Rigaku Corp. (2005)]. The structures were solved with SIR92 and refined with CRYSTALS. All non-hydrogen atoms and hydrogen atoms were refined anisotropically and isotropically, respectively. Atomic coordinates, thermal parameters, and intramolecular bond distances and angles are deposited in the Supporting Information (CIF file format).

**Kinetic Measurements.** The reaction of copper(II) complexes with  $\text{H}_2\text{O}_2$  was performed in a 1 cm path length UV-vis cell that was held in a Unisoku cryostat holder USP-203. After  $\text{CH}_3\text{CN}$  or  $\text{CH}_3\text{CH}_2\text{CN}$  solutions of copper(II) complexes (0.6 mM) in the cell was kept at a desired temperature for several minutes,  $\text{H}_2\text{O}_2$  (10 equiv) and then  $\text{Et}_3\text{N}$  (2 eq) were injected into the cell through a septa cap with use of a microsyringe. The reaction was monitored by following an increase of the characteristic absorption band of the  $\text{Cu}(\text{II})\text{-H}_2\text{O}_2$  adduct.

## Results

### Structural Characterization of Copper(II) Complexes.

First of all, the structures of the copper(II) complexes of TPA and  $\text{Ph}_n\text{TPA}$  (Chart 1) have been examined. The crystal structures of **CuTPA** and **3** have already been reported in the literature,<sup>11,12</sup> and those of **1** and **2** have newly been determined in this study as shown in Figures 1 and 2. The crystallographic data of **1** and **2** are listed in Table 1, and

**Table 1.** Summary of the X-ray Crystallographic Data of Compound **1** and **2**

compound	<b>1</b>	<b>2</b>
formula	C <sub>26</sub> H <sub>25</sub> N <sub>5</sub> CuCl <sub>2</sub> O <sub>8</sub>	C <sub>32</sub> H <sub>30</sub> N <sub>5</sub> CuCl <sub>2</sub> O <sub>8</sub>
formula weight	669.96	747.07
crystal system	monoclinic	monoclinic
space group	<i>P</i> 2 <sub>1</sub> / <i>c</i> (No. 14)	<i>P</i> 2 <sub>1</sub> / <i>n</i> (No. 14)
<i>a</i> , Å	10.585(6)	14.696(8)
<i>b</i> , Å	10.625(5)	11.748(6)
<i>c</i> , Å	24.121(19)	18.660(14)
α, deg	90	90
β, deg	95.73(4)	99.98(2)
γ, deg	90	90
<i>V</i> , Å <sup>3</sup>	2699.2 (30)	3172.9 (33)
<i>Z</i>	4	4
<i>F</i> (000)	1372.00	1536.00
<i>D</i> <sub>calcd</sub> , g/cm <sup>−3</sup>	1.649	1.564
<i>T</i> , K	153	153
crystal size, mm	0.50 × 0.50 × 0.30	0.30 × 0.20 × 0.10
μ(Mo Kα), cm <sup>−1</sup>	10.679	9.176
2θ <sub>max</sub> , deg	55.0	55.0
no. of reflns measd	25191	28922
no. of reflns obsd	5071 ( <i>I</i> > 2.00σ( <i>I</i> ))	4744 ( <i>I</i> > 0.8σ( <i>I</i> ))
no. of variables	404	460
<i>R</i> <sup>a</sup>	0.0500	0.0343
<i>R</i> <sub>w</sub> <sup>b</sup>	0.0632	0.0422
GOF	0.995	0.947

$$^a R = \sum ||F_o| - |F_c|| / \sum |F_o|. \quad ^b R_w = [\sum w(|F_o| - |F_c|)^2 / \sum w F_o^2]^{1/2}.$$

their selected bond lengths and angles are summarized in Table 2 together with those of reported **CuTPA**<sup>12</sup> and **3**<sup>11</sup> for comparison. The copper center in **1** exhibits a slightly distorted square pyramidal geometry ( $\tau = 0.12$ ),<sup>19</sup> where two pyridine nitrogen atoms N(1) and N(2), tertiary amine nitrogen atom N(3), and the acetonitrile nitrogen atom N(5) occupy each corner of the equatorial plane and the pyridine nitrogen atom N(4) of <sup>Ph</sup>Py (6-phenylpyridin-2-yl) group exists at the axial position. On the other hand, copper(II) complex **2** carrying two <sup>Ph</sup>Py groups exhibits an intermediate structure between square pyramidal and trigonal bipyramidal ( $\tau = 0.58$ ) as shown in Figure 2. Since other copper(II)-complexes **CuTPA** and **3** show trigonal bipyramidal structure ( $\tau = 0.90$  and 1.0, respectively),<sup>11,12</sup> it is obvious that the 6-Ph substituent(s) largely affect the solid state structure of the copper(II) complexes.

It should be noted that the average distance between Cu and <sup>Ph</sup>Py-nitrogen (2.159 Å) is significantly longer than the average distance between Cu and Py-nitrogen (2.015 Å). This can be attributed to the steric repulsion between the bound Cu<sup>II</sup> ion and the 6-Ph and/or that between the bound CH<sub>3</sub>CN coligand and the 6-Ph.

The ESR parameters of the copper(II) complexes determined by the computer simulation are summarized in Table 3. The ESR spectra themselves are presented in Supporting Information, Figures S1–S4. In spite of having the different structures in the solid state [square pyramidal (SP) vs trigonal bipyramidal (TBP), see above], all copper(II) complexes exhibit relatively similar ESR parameters in frozen CH<sub>3</sub>CN solution. This clearly indicates that they adopt a similar structure in solution. Judging from the relatively small *A*<sub>1</sub> values (90–130 G), they may have a trigonal bipyramidal structure as in the case of **CuTPA** and **3** in crystal. This

**Table 2.** Selected Bond Lengths (Å) and Angles (deg) of Compounds **CuTPA**, **1**, **2**, and **3**<sup>a</sup>

Compound <b>CuTPA</b> <sup>12</sup>			
Cu(1)–N(1)	2.027(4)	Cu(1)–N(2)	2.054(4)
Cu(1)–N(3)	2.007(4)	Cu(1)–N(4)	2.045(4)
Cu(1)–N(5)	1.960(4)		
N(1)–Cu(1)–N(2)	117.95(17)	N(1)–Cu(1)–N(3)	82.46(16)
N(1)–Cu(1)–N(4)	123.60(17)	N(1)–Cu(1)–N(5)	97.57(17)
N(2)–Cu(1)–N(3)	82.65(17)	N(2)–Cu(1)–N(4)	113.19(17)
N(2)–Cu(1)–N(5)	99.15(18)	N(3)–Cu(1)–N(4)	81.97(17)
N(3)–Cu(1)–N(5)	177.92(19)	N(4)–Cu(1)–N(5)	96.31(19)
Compound <b>1</b>			
Cu(1)–N(1)	1.962(2)	Cu(1)–N(2)	1.989(2)
Cu(1)–N(3)	2.042(2)	Cu(1)–N(4)	2.330(2)
Cu(1)–N(5)	1.986(2)		
N(1)–Cu(1)–N(2)	164.59(8)	N(1)–Cu(1)–N(3)	83.67(8)
N(1)–Cu(1)–N(4)	100.53(8)	N(1)–Cu(1)–N(5)	98.28(9)
N(2)–Cu(1)–N(3)	82.69(8)	N(2)–Cu(1)–N(4)	84.79(8)
N(2)–Cu(1)–N(5)	94.26(9)	N(3)–Cu(1)–N(4)	82.57(7)
N(3)–Cu(1)–N(5)	171.86(8)	N(4)–Cu(1)–N(5)	104.78(8)
Compound <b>2</b>			
Cu(1)–N(1)	2.232(2)	Cu(1)–N(2)	2.067(2)
Cu(1)–N(3)	2.000(2)	Cu(1)–N(4)	2.010(2)
Cu(1)–N(5)	1.953(2)		
N(1)–Cu(1)–N(2)	108.27(9)	N(1)–Cu(1)–N(3)	78.28(9)
N(1)–Cu(1)–N(4)	103.14(9)	N(1)–Cu(1)–N(5)	105.68(10)
N(2)–Cu(1)–N(3)	80.18(10)	N(2)–Cu(1)–N(4)	140.69(9)
N(2)–Cu(1)–N(5)	97.36(10)	N(3)–Cu(1)–N(4)	83.74(10)
N(3)–Cu(1)–N(5)	175.89(9)	N(4)–Cu(1)–N(5)	96.29(10)
Compound <b>3</b> <sup>11</sup>			
Cu(1)–N(1)	2.108(5)	Cu(1)–N(2)	2.124(7)
Cu(1)–N(3)	1.996(6)	Cu(1)–N(4)	2.091(6)
Cu(1)–N(5)	1.935(6)		
(1)–Cu(1)–N(2)	117.3(2)	N(1)–Cu(1)–N(3)	80.0(2)
N(1)–Cu(1)–N(4)	118.6(2)	N(1)–Cu(1)–N(5)	99.1(2)
N(2)–Cu(1)–N(3)	81.3(2)	N(2)–Cu(1)–N(4)	116.0(2)
N(2)–Cu(1)–N(5)	98.2(2)	N(3)–Cu(1)–N(4)	80.1(2)
N(3)–Cu(1)–N(5)	178.7(2)	N(4)–Cu(1)–N(5)	101.2(2)

<sup>a</sup> The data are taken from the literatures; ref 12 for **CuTPA** and ref 11 for **3**.

**Table 3.** Redox Potential, UV-vis, and ESR Parameters of **CuTPA**, **1**, **2**, and **3**

complex	<i>E</i> <sub>1/2</sub> (V) <sup>a</sup>	Δ <i>E</i> <sub>p</sub> (V) <sup>b</sup>	λ <sub>max</sub> (ε, M <sup>−1</sup> cm <sup>−1</sup> )	ESR parameters <sup>c</sup>	
<b>CuTPA</b>	−0.34	0.10	628 nm (85) 855 nm (300)	<i>g</i> <sub>1</sub> = 2.170 <i>g</i> <sub>2</sub> = 2.068 <i>g</i> <sub>3</sub> = 2.145	<i>A</i> <sub>1</sub> = 100 G <i>A</i> <sub>2</sub> = 30 G <i>A</i> <sub>3</sub> = 30 G
<b>1</b>	−0.28	0.08	625 nm (95) 820 nm (180)	<i>g</i> <sub>1</sub> = 2.235 <i>g</i> <sub>2</sub> = 2.043 <i>g</i> <sub>3</sub> = 2.090	<i>A</i> <sub>1</sub> = 100 G <i>A</i> <sub>2</sub> = 5 G <i>A</i> <sub>3</sub> = 30 G
<b>2</b>	−0.16	0.08	630 nm (100) 800 nm (300)	<i>g</i> <sub>1</sub> = 2.230 <i>g</i> <sub>2</sub> = 2.040 <i>g</i> <sub>3</sub> = 2.140	<i>A</i> <sub>1</sub> = 130 G <i>A</i> <sub>2</sub> = 18 G <i>A</i> <sub>3</sub> = 18 G
<b>3</b>	−0.04	0.08	650 nm (65) 865 nm (380)	<i>g</i> <sub>1</sub> = 2.185 <i>g</i> <sub>2</sub> = 2.110 <i>g</i> <sub>3</sub> = 2.120	<i>A</i> <sub>1</sub> = 90 G <i>A</i> <sub>2</sub> = 2 G <i>A</i> <sub>3</sub> = 22 G

<sup>a</sup> In CH<sub>3</sub>CN containing 0.1 M tetrabutylammonium perchlorate (TBAP) at 25 °C; working electrode Pt, counter electrode Pt, reference electrode Ag/0.01 M AgNO<sub>3</sub>, sweep rate 50 mV s<sup>−1</sup>. <sup>b</sup> Peak separation. <sup>c</sup> In CH<sub>3</sub>CN at 128–129 K, microwave frequency 9.40–9.41 GHz, modulation frequency 100 kHz, modulation amplitude 5 G, microwave power 0.32–0.33 mW.

notion is supported by the absorption spectral data presented in Table 3. Namely, two distinctive d-d bands at ~630 nm and ~850 nm of all complexes in CH<sub>3</sub>CN are indicative of a large contribution of trigonal bipyramidal (TBP) geometry in solution.<sup>20</sup>

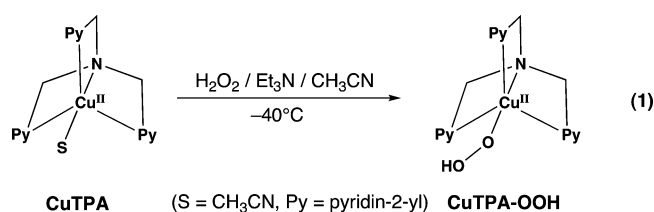
(19) Addison, A. W.; Rao, T. N.; Reedijk, J.; van Rijn, J.; Verschoor, G. C. *J. Chem. Soc., Dalton Trans.* **1984**, 1349–1356.

(20) Mukherjee, R. In *Comprehensive Coordination Chemistry II*; McCleverty, J. A.; Meyer, T. J., Eds.; Elsevier: Amsterdam, 2004; Vol. 6, pp 747–910, and references cited therein.



**Redox Potential of Copper(II) Complexes.** The redox potential of the complex is an important indicator of the electron-donor ability of the supporting ligand. The cyclic voltammograms of the complexes were measured under the same experimental conditions (Supporting Information, Figures S5–S8). In all cases, a reversible  $\text{Cu}^{\text{II}}/\text{Cu}^{\text{I}}$  redox couple was obtained, from which the redox potentials ( $E_{1/2}$ ) of the copper(II) complexes were determined as the midpoint of the oxidation and reduction peaks as summarized in Table 3. Apparently, the redox potential of the complexes largely increases in the order of  $\text{CuTPA} < \mathbf{1} < \mathbf{2} < \mathbf{3}$ . This can be attributed to the weaker electron-donor ability of the  $\text{PhPy}$  group. Namely, the steric repulsion between the bulky 6-Ph substituent and the bound copper(II) ion and/or the repulsion between the 6-Ph substitutes and the  $\text{CH}_3\text{CN}$  coligand weakens the coordinative interaction between the metal ion and  $\text{PhPy}$ -nitrogen. In addition, electron-withdrawing nature of 6-Ph may also reduces the electron donor ability of  $\text{PhPy}$ . Thus, increasing number ( $n$ ) of  $\text{PhPy}$  resulted in the reduction of the overall electron-donating nature of the TPA derivatives. The reduction in the local dielectric character because of the steric shielding of the metal center may also cause the positive shift in  $E_{1/2}$  as discussed previously.<sup>11</sup>

**Reaction of Copper(II) Complexes and  $\text{H}_2\text{O}_2$ .** Masuda and co-workers reported that the reaction of **CuTPA** and  $\text{H}_2\text{O}_2$  gave a mononuclear copper(II)-hydroperoxo complex **CuTPA-OOH** in the presence of triethylamine (eq 1).<sup>12</sup> The hydroperoxo complex exhibited a ligand-to-metal charge transfer (LMCT) band at 379 nm ( $\epsilon = 1700 \text{ M}^{-1} \text{ cm}^{-1}$ ) together with d-d bands at 668 nm ( $170 \text{ M}^{-1} \text{ cm}^{-1}$ ) and 828 nm ( $200 \text{ M}^{-1} \text{ cm}^{-1}$ ),<sup>12</sup> and the ESR parameters of  $g_{\parallel} = 2.01$ ,  $g_{\perp} = 2.19$ ,  $A_{\parallel} = 87 \text{ G}$ , and  $A_{\perp} = 99 \text{ G}$ . These spectral data indicate that **CuTPA-OOH** has a trigonal bipyramidal structure as in the case of the starting material.<sup>12</sup> Furthermore, **CuTPA-OOH** showed a resonance Raman band at  $847 \text{ cm}^{-1}$  assignable to the  $^{16}\text{O}-^{16}\text{O}$  stretching vibration, which shifted to  $792 \text{ cm}^{-1}$  upon  $^{18}\text{O}$ -substitution.<sup>12</sup>



In this study, reactions of other copper(II) complexes and  $\text{H}_2\text{O}_2$  have been examined under similar experimental conditions. Figure 3 shows the spectral change for the reaction of complex **1** and  $\text{H}_2\text{O}_2$  (10 equiv) in  $\text{CH}_3\text{CN}$  at  $-40^\circ\text{C}$  in the presence of 2 equiv of  $\text{Et}_3\text{N}$ , where an absorption band at 384 nm ( $\epsilon = 1550 \text{ M}^{-1} \text{ cm}^{-1}$ ) appears together with a d-d band at 620 nm ( $170 \text{ M}^{-1} \text{ cm}^{-1}$ ). In this case, the resonance Raman spectrum of the resulting solution exhibited a peak at  $840 \text{ cm}^{-1}$  attributable to the  $^{16}\text{O}-^{16}\text{O}$  stretching vibration of a hydroperoxo species, although the Raman band of the  $^{18}\text{O}$ -derivative was difficult to detect because of its weak intensity (inset of Figure 3). The UV-vis and the resonance Raman data are very close to those of

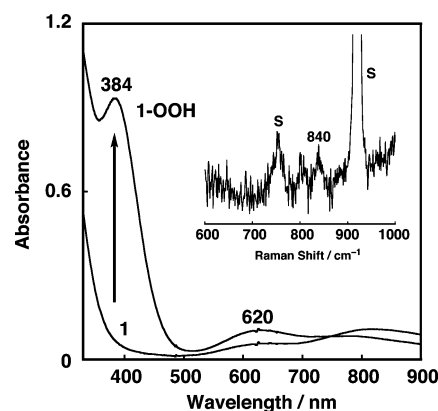
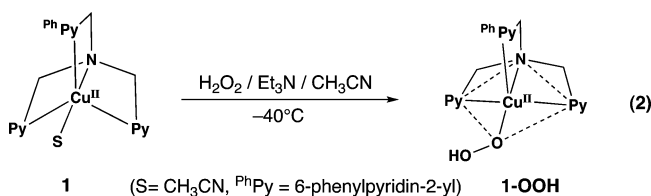


**Figure 3.** Spectral change for the reaction of **1** (0.6 mM) with  $\text{H}_2\text{O}_2$  (6.0 mM) in the presence of  $\text{NEt}_3$  (1.2 mM) in  $\text{CH}_3\text{CN}$  at  $-40^\circ\text{C}$ . Inset: Resonance Raman spectrum of **1-OOH** (6 mM) generated by the reaction of **1** and  $\text{H}_2^{16}\text{O}_2$  in  $\text{CH}_3\text{CN}$  at  $-40^\circ\text{C}$  ( $\lambda_{\text{ex}} = 406.7 \text{ nm}$ ); s denotes the solvent bands.

**CuTPA-OOH**, confirming that the generated species is also a copper(II)-hydroperoxo complex **1-OOH** (eq 2).

The ESR spectrum of **1-OOH** shown in Supporting Information, Figure S9 exhibits a larger  $A_{\parallel}$  value (166 G) as compared with that of the starting material **1** (100 G), suggesting that the trigonal bipyramidal structure of **1** in solution becomes a distorted square pyramidal structure in **1-OOH**. This notion is supported by the UV-vis spectral change shown in Figure 3, where the relatively intense d-d band at 820 nm of **1**, which is a characteristic d-d band for copper(II) complexes with trigonal bipyramidal structure, is diminished in **1-OOH**. Binding of the stronger electron-donating ligand like  $\text{HOO}^-$  to copper(II) center shifts its position from the axial of trigonal bipyramidal geometry to the equatorial of square pyramidal structure as illustrated in eq 2. Moreover, double integration of the ESR spectrum of **1-OOH** demonstrated that 99% of the spin remained, confirming the mononuclearity of **1-OOH**.



The reaction of **2** and  $\text{H}_2\text{O}_2$  was then examined in propionitrile at  $-70^\circ\text{C}$  in the presence of  $\text{Et}_3\text{N}$ . The spectral change of the reaction is shown in Figure 4, where an intense absorption band at 379 nm ( $\epsilon = 6200 \text{ M}^{-1} \text{ cm}^{-1}$ ) readily appears.<sup>21</sup> Notably, the spectrum is different from that of the mononuclear copper(II) hydroperoxo complex **1-OOH** shown in Figure 3, and the generated intermediate was ESR silent. The resonance Raman spectrum measured at  $-80^\circ\text{C}$  with  $\lambda_{\text{ex}} = 406.7 \text{ nm}$  exhibited a characteristic peak at  $607 \text{ cm}^{-1}$  that shifted to  $577 \text{ cm}^{-1}$  upon  $\text{H}_2^{18}\text{O}_2$  substitution (inset of Figure 4). All these spectral characteristics are very close

(21) The reaction of  $\text{H}_2\text{O}_2$  and **2** in  $\text{CH}_3\text{CN}$  at  $-40^\circ\text{C}$  gave the same spectrum as shown in Supporting Information, Figure S10.

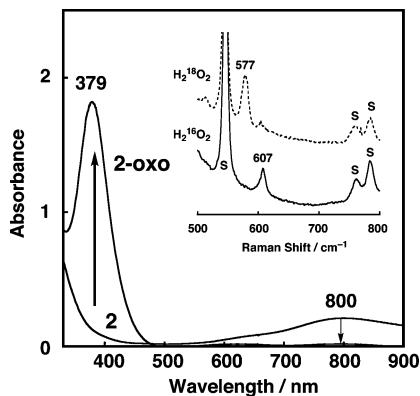


**Figure 4.** Spectral change for the reaction of **2** (0.6 mM) and H<sub>2</sub>O<sub>2</sub> (6.0 mM) in the presence of NEt<sub>3</sub> (1.2 mM) in CH<sub>3</sub>CH<sub>2</sub>CN at -70 °C. Inset: Resonance Raman spectra of **2-oxo** (6 mM) generated by using H<sub>2</sub><sup>16</sup>O<sub>2</sub> (solid line) and H<sub>2</sub><sup>18</sup>O<sub>2</sub> (dashed line) with excitation at λ<sub>ex</sub> = 406.7 nm in CH<sub>3</sub>CH<sub>2</sub>CN at -80 °C; s denotes the solvent bands.

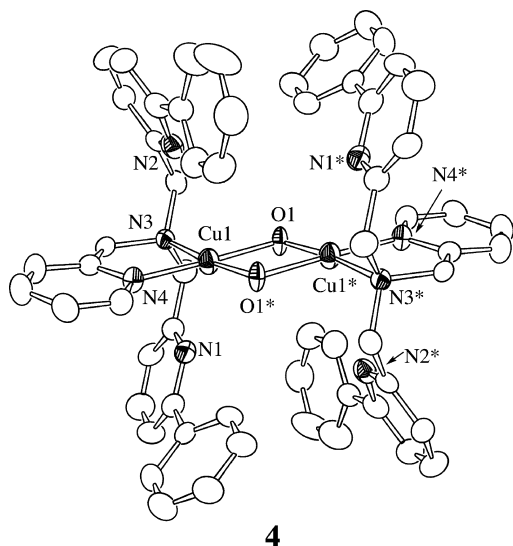
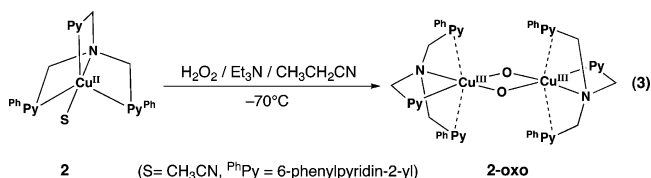


**Figure 5.** ORTEP drawing of **4** showing 50% probability thermal ellipsoids. The counteranion and the hydrogen atoms are omitted for clarity.

to those of the reported bis(μ-oxo)dicopper(III) complexes,<sup>22</sup> strongly suggesting the formation of a similar complex **2-oxo** as indicated in (eq 3).



At first glance, it seems to be difficult to assess such a doubly bridged dinuclear copper complex using the sterically demanding ligand Ph<sub>2</sub>TPA, but such a possibility has been realized by the formation of bis(μ-hydroxo)dicopper(II) complex **4** (Figure 5) in the treatment of **2** with Et<sub>3</sub>N in MeOH. The crystallographic data and the selected bond

**Table 4.** Summary of the X-ray Crystallographic Data of Compound **4**

compound	<b>4</b>
formula	C <sub>31</sub> H <sub>26</sub> N <sub>4</sub> CuF <sub>3</sub> O <sub>4</sub> S
formula weight	671.17
crystal system	triclinic
space group	<i>P</i> $\bar{1}$ (No. 2)
<i>a</i> , Å	11.700(8)
<i>b</i> , Å	12.320(9)
<i>c</i> , Å	12.710(10)
α, deg	106.76(2)
β, deg	107.09(2)
γ, deg	112.149(20)
<i>V</i> , Å <sup>3</sup>	1447.9(18)
<i>Z</i>	2
<i>F</i> (000)	688.0
<i>D</i> <sub>calcd</sub> , g/cm <sup>-3</sup>	1.539
<i>T</i> , K	153
crystal size, mm	0.30 × 0.30 × 0.20
μ(Mo Kα), cm <sup>-1</sup>	8.906
2θ <sub>max</sub> , deg	55.0
no. of refls measd	14207
no. of refls obsd	4252([ <i>I</i> > 0.50σ( <i>I</i> )])
no. of variables	423
<i>R</i> <sup>a</sup>	0.0450
<i>R</i> <sub>w</sub> <sup>b</sup>	0.0497
GOF	0.974

$$^a R = \sum ||F_o| - |F_c|| / \sum |F_o|, \quad ^b R_w = [\sum w(|F_o| - |F_c|)^2 / \sum w F_o^2]^{1/2}.$$

**Table 5.** Selected Bond Lengths (Å) and Angles (deg) of Compound **4**

Compound <b>4</b>			
Cu(1)–O(1)	1.929(4)	Cu(1)–O*(1)	1.932(3)
Cu(1)–N(1)	2.924(6)	Cu(1)–N(2)	2.754(5)
Cu(1)–N(3)	2.049(5)	Cu(1)–N(4)	1.996(4)
Cu(1)–Cu*(1)	2.9983(10)		
O(1)–Cu(1)–O*(1)	78.13(17)	O(1)–Cu(1)–N(3)	173.97(15)
O(1)–Cu(1)–N(4)	100.1(2)	O(1)–Cu(1)–N(3)	97.04(19)
O(1)*–Cu(1)–N(4)	176.76(19)	N(3)–Cu(1)–N(4)	84.6(2)

lengths and angles of **4** are presented in Table 4 and Table 5, respectively.

Complex **4** consists of a centrosymmetric Cu<sub>2</sub>(μ-OH)<sub>2</sub> core supported by two Ph<sub>2</sub>TPA ligands. Each copper ion has a square planar geometry consisting of a N<sub>2</sub>O<sub>2</sub> donor set with the pyridyl nitrogen atom N(4), *tert*-amine nitrogen atom N(3), and two bridging hydroxo oxygen atoms O(1) and O(1)\*, whereas the two pyridine donor groups having the 6-Ph substituent (PhPy) interact with the copper ion very weakly from the axial position (Cu–N(1) and Cu–N(2) are 2.754 Å and 2.924 Å, respectively). Thus, the ligand Ph<sub>2</sub>TPA seems to behave as a bidentate ligand in this particular system. The overall structure of **4** is similar to that of [Cu<sub>2</sub>(OH)<sub>2</sub>(Me<sub>2</sub>-TPA)<sub>2</sub>](ClO<sub>4</sub>)<sub>2</sub> reported by Suzuki and co-workers,<sup>23</sup> but the average distances of Cu–N<sub>axial</sub> (2.839 Å) and Cu···Cu\* (2.998 Å) bonds are substantially elongated as compared with those of Suzuki's complex [Cu–N<sub>axial</sub> (2.596 Å), and Cu···Cu\* (2.936 Å)].<sup>23</sup> The larger values of Cu–N<sub>axial</sub> and Cu···Cu\* bond distances in **4** relative to those of [Cu<sub>2</sub>(OH)<sub>2</sub>(Me<sub>2</sub>-TPA)<sub>2</sub>]<sup>2+</sup> reflect the larger steric bulkiness of 6-Ph as compared with that of 6-Me.

Interestingly, complex **3** behaved quite differently in the reaction with H<sub>2</sub>O<sub>2</sub>. Namely, copper(II) complex **3** was reduced to the corresponding copper(I) complex **3<sup>red</sup>**. The

(22) (a) Que, L., Jr.; Tolman, W. B. *Angew. Chem., Int. Ed.* **2002**, *41*, 1114–1137. (b) Henson, M. J.; Mukherjee, P.; Root, D. E.; Stack, T. D. P.; Solomon, E. I. *J. Am. Chem. Soc.* **1999**, *121*, 10332–10345. (c) Holland, P. L.; Cramer, C. J.; Wilkinson, E. C.; Mahapatra, S.; Rogers, K. R.; Itoh, S.; Taki, M.; Fukuzumi, S.; Que, L., Jr.; Tolman, W. B. *J. Am. Chem. Soc.* **2000**, *122*, 792–802.

(23) Hayashi, H.; Fujinami, S.; Nagatomo, S.; Ogo, S.; Suzuki, M.; Uehara, A.; Watanabe, Y.; Kitagawa, T. *J. Am. Chem. Soc.* **2000**, *122*, 2124–2125.

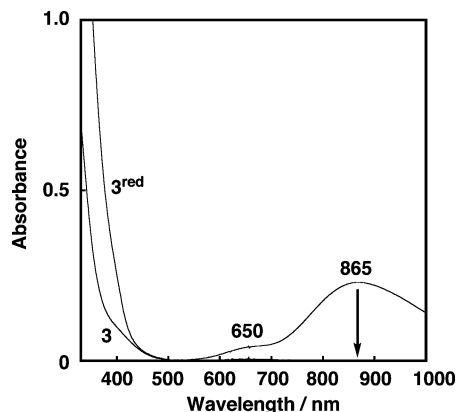


**Figure 6.** Spectral change for the reaction of **3** (0.6 mM) with  $\text{H}_2\text{O}_2$  (6.0 mM) in the presence of  $\text{Et}_3\text{N}$  (1.2 mM) in  $\text{CH}_3\text{CN}$  at  $-40^\circ\text{C}$ .

d-d bands at 650 and 865 nm of the copper(II) complex **3** completely disappeared (see Figure 6) and the resulting solution became ESR silent. The ESI-MS data and the elemental analysis on the isolated product confirmed the formation of **3<sup>red</sup>** (Supporting Information, Figure S11). The reduction of copper(II) to copper(I) in **3** may proceed via  $\text{Cu}^{\text{II}}\text{--O}$  bond homolysis of an initially formed copper(II)-hydroperoxo intermediate **3-OOH** as previously reported in a related system.<sup>24</sup>

## Discussion

In this study, substituent effects of 6-Ph on the structure, physicochemical properties, and  $\text{H}_2\text{O}_2$ -reactivity of the copper(II) complexes supported by  $\text{Ph}_n\text{TPA}$  ligands (see, Chart 1) have systematically been examined. The copper(II) centers of **CuTPA** and **3** ( $\text{Ph}_3\text{TPA}$ -complex) exhibit trigonal bipyramidal structure in the crystal, whereas complex **1** supported by  $\text{Ph}_1\text{TPA}$  shows a slightly distorted square pyramidal geometry (Figure 1). Complex **2** supported by  $\text{Ph}_2\text{TPA}$ , on the other hand, takes an intermediate structure between trigonal bipyramidal and square pyramidal in the solid state. However, the UV-vis and ESR data suggest that all copper(II) complexes exhibit a similar trigonal bipyramidal geometry in solution. Thus, the difference in the solid-state structures of the complexes can be attributed to the crystal packing force.

Copper(II) complexes **CuTPA**, **1**, **2**, and **3** have redox potential at  $-0.34$ ,  $-0.28$ ,  $-0.16$ , and  $-0.04$  V vs  $\text{Ag}/\text{AgNO}_3$ , respectively. Thus, incorporation of each 6-Ph group causes  $\sim 0.1$  V increase of  $E_{1/2}$ . The positive shift of  $E_{1/2}$  has been attributed to the steric repulsion between the bulky 6-Ph substituent and the cupric ion and/or the repulsion between the 6-Ph and the  $\text{CH}_3\text{CN}$  coligand, which cause reduction of the coordinative interaction between the pyridine donor groups and the copper(II) ion. In fact, the average distance between Cu and  $\text{PhPy}$ -nitrogen (2.159 Å) is substantially elongated as compared to the average distance between Cu and Py-nitrogen (2.015 Å) (vide ante). The electron-withdrawing effect by 6-Ph as well as a reduction of the local dielectric character because of the steric shielding in the metal center may also contribute to the positive shift of  $E_{1/2}$ .

The  $\text{Cu}(\text{II})\text{--H}_2\text{O}_2$  reactivity is drastically altered by the supporting ligands. **CuTPA** and **1** supported by TPA itself and  $\text{Ph}_1\text{TPA}$ , respectively, afforded the mononuclear copper(II)-hydroperoxo complex **CuTPA-OOH** and **1-OOH**. It should be noted here that no ligand modification (neither *N*-dealkylation nor aromatic hydroxylation) took place from these copper(II)-hydroperoxo species, even though the reaction mixture was warmed to room temperature before the workup treatment. This is in contrast to Karlin's system with a  $\text{Ph}_1\text{TPA}$  having *p*-*tert*-butyl substituent on 6-Ph, where a aromatic ligand hydroxylation reaction was observed (20%).<sup>14</sup> This can be attributed to the existence of the electron-donating *tert*-butyl substituent on 6-Ph in Karlin's system, which may increase the susceptibility of the aromatic substituent toward the electrophilic attack by the  $\text{Cu-OOH}$  moiety.

Incorporation of an extra 6-Ph group to  $\text{Ph}_1\text{TPA}$  to give  $\text{Ph}_2\text{TPA}$  resulted in totally different reactivity of the supported copper(II) complex toward  $\text{H}_2\text{O}_2$ . In this case, bis( $\mu$ -oxo)dicopper(III) complex **2-oxo** was generated. Replacement of two pyridine (Py) groups of TPA by the bulkier  $\text{PhPy}$  groups may enforce the TPA derivative to act as a bidentate ligand using the non-substituted Py group and the *tert*-amine nitrogen as the donor groups. Such a bidentate 2-pyridylmethylamine ( $\text{PyCH}_2\text{NR}_2$ ) type ligand has been well-demonstrated to stabilize the bis( $\mu$ -oxo)dicopper(III) complex.<sup>25</sup> This may be the reason why  $\text{Ph}_2\text{TPA}$  affords **2-oxo**. Suzuki and his co-workers reported that the reaction of  $[\text{Cu}^{\text{I}}(\text{Me}_2\text{TPA})]^+$  and  $\text{O}_2$  also gave a bis( $\mu$ -oxo)dicopper(III) complex, in which the copper(III) center exhibited a four-coordinate square planar geometry with a  $\text{N}_2\text{O}_2$  donor set (consisting of Py nitrogen, *tert*-amine nitrogen, and two oxo groups) and the remaining  $\text{MePy}$  groups interact with copper(III) ion very weakly from the axial positions.<sup>23</sup>

In the case of **2-oxo**, *N*-dealkylation reaction took place to give 6-phenyl-2-pyridinecarboxaldehyde in 36%. However, we did not see any ligand modification on the 6-Ph aromatic group. This is in contrast to Suzuki's  $\text{Me}_2\text{TPA}$  system, where they observed peroxygenation of the 6-Me substituent in the reaction of  $[\text{Cu}^{\text{I}}(\text{Me}_2\text{TPA})]^{2+}$  complex and  $\text{H}_2\text{O}_2$ .<sup>26</sup>

Because of the high  $E_{1/2}$  of the  $\text{Ph}_3\text{TPA}$  system, on the other hand, the copper(II) complex **3** was easily reduced to the corresponding copper(I) complex by the reaction with  $\text{H}_2\text{O}_2$ . The reaction may proceed via  $\text{Cu}\text{--O}$  bond homolysis of an initially formed  $\text{Cu}^{\text{II}}\text{--OOH}$  intermediate.

Although the factors that control the  $\text{H}_2\text{O}_2$ -reactivity of the supported copper(II) complexes have yet to be clarified completely, the results reported herein will provide important insights into the aromatic substituent effects on the redox chemistry of the TPA-complexes.

(24) Osako, T.; Nagatomo, S.; Tachi, Y.; Kitagawa, T.; Itoh, S. *Angew. Chem., Int. Ed.* **2002**, *41*, 4325–4328.

(25) (a) Holland, P. L.; Rodgers, K. R.; Tolman, W. B. *Angew. Chem., Int. Ed.* **1999**, *38*, 1139–1142. (b) Shimokawa, C.; Teraoka, J.; Tachi, Y.; Itoh, S. *J. Inorg. Biochem.* **2006**, *100*, 1118–1127.

(26) Mizuno, M.; Honda, K.; Cho, J.; Furutachi, H.; Tosha, T.; Matsumoto, T.; Fujinami, S.; Kitagawa, T.; Suzuki, M. *Angew. Chem., Int. Ed.* **2006**, *45*, 6911–6914.

**Acknowledgment.** This work was financially supported in part by Grants-in-Aid for Scientific Research on Priority Area (Nos. 19020058, 20036044, and 20037057 for S.I.) and Global Center of Excellence (GCOE) Program (“Picobiology: Life Science at Atomic Level” to T.O.) from MEXT, Japan and by Grants-in-Aid for Scientific Research (No. 20350082 for S.I.) from JSPS, Japan. The authors also thank Asahi Glass Foundation for the financial support and JSPS Research Fellowship (for A.K.).

**Supporting Information Available:** The ESR spectra (Figures S1–S4) and the cyclic voltammograms (Figures S5–S8) of the copper(II) starting materials, the ESR spectrum of **1-OOH** (Figure S9), UV–vis spectrum of **2-oxo** generated by using H<sub>2</sub>O<sub>2</sub> in CH<sub>3</sub>CN (Figure S10), and ESI-MS of **3<sup>red</sup>** generated by the reaction of **3** and H<sub>2</sub>O<sub>2</sub> in CH<sub>3</sub>CN. (Figure S10). This material is available free of charge via the Internet at <http://pubs.acs.org>.

IC801568G